

AGN and Star Formation Feedback in Galaxy Outflows

Elisabete M. de Gouveia Dal Pino¹, William Clavijo-Bohórquez¹
and Claudio Melioli²

¹Instituto de Astronomia, Geofísica e Ciências Atmosféricas (IAG), Universidade de São Paulo, CEP 05508-090, São Paulo, Brazil
emails: dalpino@iag.usp.br, weclavijob@usp.br

²University of Modena, Italy

Abstract. Large-scale, broad outflows are common in active galaxies. In systems where star formation coexists with an AGN, it is unclear yet the role that both play on driving the outflows. In this work we present three-dimensional radiative-cooling MHD simulations of the formation of these outflows, considering the feedback from both the AGN and supernovae-driven winds. We find that a large-opening-angle AGN wind develops fountain structures that make the expanding gas to fallback. Furthermore, it exhausts the gas near the nuclear region, extinguishing star formation and accretion within a few 100.000 yr, which establishes the duty cycle of these outflows. The AGN wind accounts for the highest speed features in the outflow with velocities around 10.000 km s^{-1} (as observed in UFOs), but these are not as cold and dense as required by observations of molecular outflows. The SNe-driven wind is the main responsible for the observed mass-loading of the outflows.

Keywords. Galaxy: active, Star Formation, Supernova

1. Introduction

Fast massive, poorly collimated outflows of HI and molecular gas, with velocities $\sim 600\text{-}1500 \text{ km s}^{-1}$, have been recently observed in the central regions of AGN sources like Seyfert galaxies and ULIRGs (e.g. [Morganti et al. 2005, 2013](#); see also R. Morganti in these procs.). Also, much hotter ultra-fast outflows (UFOs) with velocities $\sim 0.03\text{-}0.3c$ have been detected in X-rays (e.g. [Tombesi et al. 2013](#)). An interesting example of a molecular outflow is the ULIRG AGN 4C12.50. It exhibits HI and CO gas outflow with velocity $\sim 1000 \text{ km s}^{-1}$ which is co-spatial with the radio jet hot-spot, at 100 pc scales ([Morganti et al. 2013, 2014, Dasyra & Combes 2012](#)). This is probably produced by radiative cooling of shocked gas due to jet interaction with the ISM. Typically, gas column densities $\sim 10^{21} - 10^{22} \text{ cm}^{-2}$ are inferred for these outflows, mass loss rates up to $100 \text{ M}_\odot \text{ yr}^{-1}$, and HI clumps with mass larger than 600 M_\odot . A spectacular example of UFO is the one detected (in X-rays) in the Seyfert NGC 4151 central region, denominated Eye of Sauron, which is surrounded by ionized hydrogen (HII) associated to star formation regions observed in optical and is also connected with infalling HI gas observed in radio with VLA ([Wang et al. 2010](#)). UFOs have even larger column densities $\sim 10^{23} - 10^{24} \text{ cm}^{-2}$ ([Kraemer et al. 2018](#)).

The investigation of these outflows is important as they transport energy and gas outwards from the central regions and may affect the evolution of the host galaxy and its surrounds as well. Their origin is not yet fully understood, but the accreting supermassive black hole (SMBH) in the center of the AGN is believed to be their main driving

source. Injection mechanisms such as radiation pressure, or the kinetic interaction of the radio plasma with the ISM, or even magneto-centrifugal processes are often invoked (e.g. Kremer et al 2018 and references therein). A key point when investigating these outflows is the fact that they are generally associated with Seyferts, for which SF regions and starbursts (SB) coexist with the AGN, and the energy power emitted by both the nuclear AGN and the host galaxy is comparable, so that it is unclear the relative role of the SF and the AGN on the driving of the outflows ([Melioli & de Gouveia Dal Pino 2015](#)).

In this work, we explore the formation and evolution of these outflows in a Seyfert-like galaxy (within 1 kpc scale) by means of 3D MHD simulations at high resolution (3.9 pc) including gas radiative cooling, magnetic fields and the mechanical feedback from both SF (through the production of type Ia and II SNe) and AGN outflows.

2. Results of the MHD Simulations

For the numerical setup of our simulations, we have considered a total gravitational potential provided by dark matter, the galactic bulge and the disk. We adopted a black hole to bulge mass ratio 10^{-3} and considered a multi-phase, initially stratified gas disk supported both by rotation, and thermal and magnetic pressures. We have considered a SF rate of $1 \text{ M}_\odot \text{ yr}^{-1}$, type Ia SNe rate = 0.01 yr^{-1} and type II SNe rate 0.1 yr^{-1} . We have considered equilibrium radiative cooling for a gas able to achieve temperatures between $T = 100 \text{ K}$ to 10^8 K . We have taken initial thermal to magnetic pressures $\beta \equiv \infty$, =300, 30, 3, column densities 10^{22} to 10^{23} cm^{-2} , AGN wind initial aperture angles = 0° , 10° , or spherical, with injection power $10^{43} \text{ erg s}^{-1}$, velocity $v = 0.06c$ and mass rate $5 \times 10^{-4} \text{ M}_\odot \text{ yr}^{-1}$. (For more details see [Melioli & de Gouveia Dal Pino 2015](#); Clavijo-Bohórquez, de Gouveia Dal Pino and Melioli, in prep.).

As an example, Figure compares four evolved models at $t = 5 \text{ Myr}$. These diagrams clearly indicate that a larger AGN outflow opening angle has a major influence on the nuclear region evolution, sweeping the ISM matter, dragging the SN-driven winds, quenching accretion and star formation, and accelerating much more gas to velocities above 10.000 km s^{-1} . The comparison of the results for the two different initial magnetic field geometries do not reveal substantial differences, this in part because of the large value adopted for β here (which is compatible to the values expected from observations at these scales). Nevertheless, the comparison of the velocity-density diagrams with pure HD simulations indicate that the presence of B helps to preserve and increase the number of denser structures at higher (positive and negative) velocities.

Our simulations also show that the winds driven by the products of SF alone (i.e., by explosions of supernovae, SNe) can drive outflows with velocities $\sim 100 - 1000 \text{ km s}^{-1}$ and mass outflow rates of the order of $50 \text{ M}_\odot \text{ yr}^{-1}$ (Figure, which resemble the properties of warm absorbers (WAs) and molecular outflows. However, the resulting densities ($\sim 1 - 10 \text{ cm}^{-3}$) and temperatures (between 10^4 and 10^5 K) are too low and too high, respectively, compared to the expected values of these outflows.

The presence of an AGN-wind, particularly with large opening angle, causes the formation of fountain-like structures (Fig. 1) that make part of the expanding gas (pushed also by the SF-wind) to fallback, producing a “positive” feedback on the host galaxy evolution. This effect is more pronounced in presence of magnetic fields, due to the action of extra magnetic forces by the AGN. This reduces the mass loss rate in the outflows by factors up to 10 when compared with HD models (see Figure 2).

Figure 3 depicts the early evolution ($t \sim 950.000 \text{ yr}$) for a model with an AGN-wind injected spherically in the nucleus, after the SNe-driven wind is entirely developed. We note that the wind is quickly collimated by the surrounding gas forming dipolar outflows that resemble UFOs. The diagrams and the density-velocity histogram show

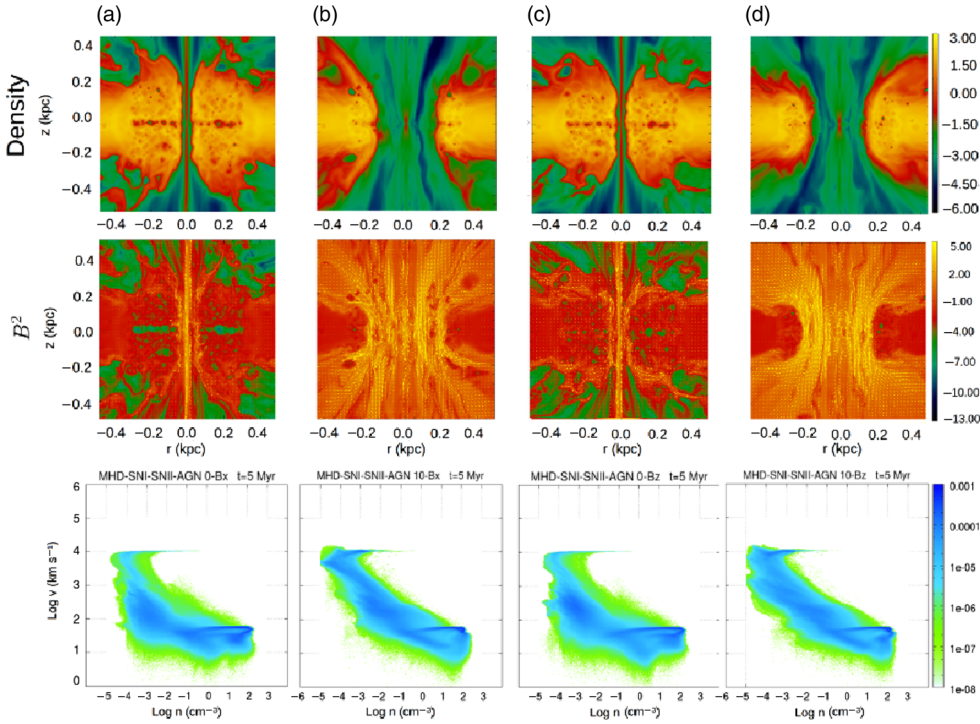


Figure 1. Top: Two-dimensional (2D) central cuts of the density distribution within one-kpc region of the evolved galaxy (at 5 Myr), for four different initial conditions. From left to right: (a) a system with initial homogeneous horizontal magnetic field ($\beta = 300$, and $B_x = 0.76\mu\text{G}$) and an AGN outflow with 0° opening angle (collimated); (b) the same as in the left panel, but with the AGN outflow with 10° opening angle; (c) the same as in (a), but with initial homogeneous vertical magnetic field (B_z); and (d) the same as in (c), but with the AGN outflow with 10° opening angle. Middle: 2D central cuts of the magnetic field strength (B^2), with the magnetic field vectors superposed to it. Bottom: 2D histograms of the vertical velocity versus density distribution, calculated considering all the cells of the systems. Velocity is in km s^{-1} and density in cm^{-3} , both in logarithmic scale. The color bar indicates the cell numbers normalized to their total number (see more details in Clavijo-Bohórquez, de Gouveia Dal Pino, Melioli in prep.).

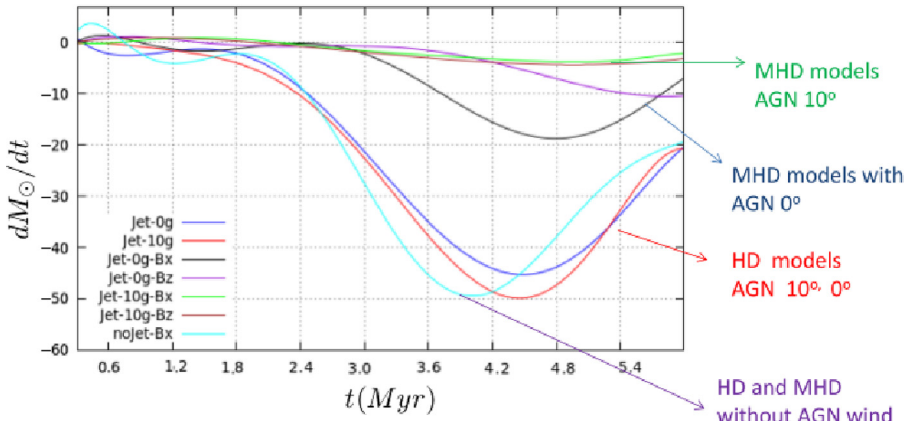


Figure 2. Time evolution of total gas mass loss rate from the thick disk of the galaxy ($|z| \leq 200$ pc) for different models as indicated by the colors (see more details in Clavijo-Bohórquez, de Gouveia Dal Pino, Melioli in prep.).

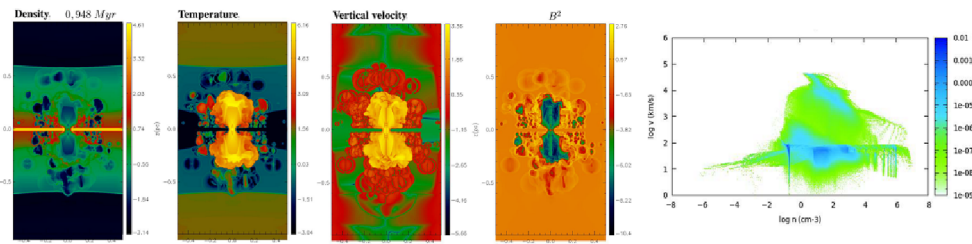


Figure 3. Early evolution for a model with an AGN wind injected spherically in the nuclear region with initial power 2×10^{45} erg s $^{-1}$, mass rate $1.5 \text{ M}_\odot \text{ yr}^{-1}$, and velocity 0.21 c. From left to right: 2D cuts of density, temperature, velocity and magnetic field strength distributions; and velocity-density histogram as in Figure 1 (see more details in Clavijo-Bohórquez, de Gouveia Dal Pino, Melioli in prep.).

that high speed, dense structures with velocities larger than 10.000 km s $^{-1}$, temperatures $> 10^7$ K, and densities $> 100 \text{ cm}^{-3}$ do develop. Besides, intermediate speed structures are also detected with velocities $\sim 1000 \text{ km s}^{-1}$, temperatures $> 1000 \text{ K}$, and densities $< 10^6 \text{ cm}^{-3}$.

3. Discussion and Conclusions

MHD radiative cooling simulations of the nuclear region (1 kpc 3 scale) of Seyfert-like galaxies, taking into account both the SF and AGN outflow feedback, result the following:

The SNe can drive outflows with velocities of a few 1000 km/s, but the characteristic densities are too low and the temperatures too large in comparison to the observations of WA and molecular outflows.

A collimated AGN jet alone (without SNe-driven wind) is unable to drive massive outflows, but can accelerate structures to very high speeds (as observed in UFOs).

An AGN wind with large opening angle sweeps more ISM matter, accelerates more gas to $v > 10.000 \text{ km s}^{-1}$, but it exhausts gas fuel and quenches accretion onto the SMBH and star formation in the nuclear regions within a few 100.000 yr. This indicates that the duty cycle of these outflows is around a few 100.000 yr, which is compatible with the timescales inferred for the observed UFOs and molecular outflows.

Mass loss rates up to $50 \text{ M}_\odot \text{ yr}^{-1}$ (which are compatible with the observations of molecular outflows) are driven mainly by the SNe-driven-wind component.

Large opening angle AGN-winds, specially in MHD flows, favor the fallback of gas to the galaxy (fountain) which decreases the mass loss rate.

An AGN spherical wind injected when the SNe wind is fully developed improves the results, producing UFO characteristics ($v > 10.000 \text{ km s}^{-1}$, $T > 10^7 \text{ K}$, and $n > 100 \text{ cm}^{-3}$), but the slower outflow component with $v \sim 1000 \text{ km s}^{-1}$ is too hot to explain the molecular outflows.

Missing ingredient in our models, like the presence of non-equilibrium ionization radiative cooling to account for more efficient coolers (molecules and dust) that could survive to evaporation and destruction in interactions with high speed hot gas, will help to improve our results and ensure the survival of the cold, dense clumpy structures that are swept to very high speeds as observed in molecular outflows.

Acknowledgments

We acknowledge support from the Brazilian agencies FAPESP (2013/10559-5 grant) and CNPq (306598/2009-4 grant). The simulations presented in this lecture have made use of the computing facilities of the GAPAE group (IAG-USP) and the Laboratory of Astroinformatics IAG/USP, NAT/Unicsul (FAPESP grant 2009/54006-4).

References

- Dasyra, K. M & Combes, F. 2012, *A&A*, 541, L7
- Amari, S., Hoppe, P., Zinner, E., & Lewis R.S. 1995, *ApJ*, 30, 490
- Kraemer, S. B., Tombesi, F., & Bottorff M. C. 2018, *ApJ*, 852, 35
- Melioli, C., & de Gouveia Dal Pino, E. M. 2015, *ApJ*, 812, 90
- Morganti, R., Oosterloo, T. A., Tadhunter, C. N., van Moorsel, G., & Emonts, B., 2005 *A&A*, 439, 521
- Morganti, R., Frieswijk, W., Oonk, R. J. B., Oosterloo, T., & Tadhunter, C. 2013, *A&A*, 552, L4
- Morganti, R., Oosterloo, T. A., Oonk, J. B. R., Frieswijk, W., & Tadhunter, C. N. 2015, *ASP-CS*, 499, 125
- Oosterloo, T. A., Morganti, R., Tzioumis, A., Reynolds, J., King, E., McCulloch, P., & Tsvetanov, Z. 2000, *AJ*, 119, 2085
- Tadhunter, C., Morganti, R., Rose, M., Oonk, J. B. R., & Oosterloo, T. 2014, *Nature*, 511, 440
- Tombesi, F., Cappi, M., Reeves, J. N., Palumbo, G. G. C., Braito, V., & Dadina, M. 2011, *ApJ*, 742, 44
- Tombesi, F., Cappi, M., Reeves, J. N., Nemmen, R. S., Braito, V., Gaspari, M., & Reynolds, S. 2013, *MNRAS*, 430, 1102
- Tombesi, F., Meléndez, M., Veilleux, S., Reeves, J.M., González-Alfonso, C., & Reynolds, C. S. 2015, *Nature*, 519, 436
- Wagner, A. Y., Umemura, M., & Bicknell, G. V. 2013, *ApJ*, 763, L18
- Wang, J., Fabbiano, G., Risaliti, G., Elvis, M., Mundell, C. G., Dumas, G., Schinnerer, E., & Zezas, A. 2010, *ApJ*, 719, L208